Research Article | Vol. 30, No. 11 / 23 May 2022 / Optics Express 18471
Optics EXPRESS

# Dual projectile beams

OUIS CHOUAIB BOUMEDDINE,[1,2,*] ALESSANDRO ZANNOTTI,[2] BENCHEIKH ABDELHALIM,[1,3] AND CORNELIA DENZ[2]

[1]Applied Optics Laboratory, IOMP Institute, University of Setif 1, Setif 19000, Algeria
[2]Institute of Applied Physics and Center for Nonlinear Science (CeNoS), University of Muenster, 48149 Muenster, Germany
[3]Electromechanical Department, University of BBA, BBA 34000, Algeria
[*]o.boumeddine@uni-muenster.de

**Abstract:** Accelerating beams, of which the Airy beam is an important representative, are characterized by intensity maxima that propagate along curved trajectories. In this work we present a simple approach to directly generate accelerating beams with controllable trajectories by means of binary phase structures that consist of only a $\pi$ phase step modulation in comparison to previous studies where two-dimensional cubic phase modulations for example are required, and which have practical limitations due to their challenging fabrication with phase plates or diffractive optical elements (DOEs), or the spatially extended system needed for their generation at the Fourier plane. In our approach, two intensity maxima are formed that propagate along root parabolic trajectories in contrast to Airy and higher order caustic beams that propagate along a parabolic curve, hence we call these beams Dual Projectile Beams (DPBs). By tailoring a step or slit phase patterns with additional Fresnel lenses, we either generate hollow-core or abruptly focusing beams and control their curvatures. Moreover, using DPBs as a simpler complement to complex structured light fields, we demonstrate their versatility at the example of their interaction with nonlinear matter, namely the formation of a spatial soliton in a photorefractive material. We show that the formed solitary state propagates almost unchanged for a distance of several Rayleigh lengths. This light matter interaction can be regarded as a light beam deceleration. The simplicity of this approach makes these beams suitable for integrated optics and high-power laser applications using DOEs or meta-surfaces.



## 1. Introduction

The Airy wave packet, introduced by Berry and Balazs in 1979 [1], is a solution of the Schrödinger equation for a linear potential that has an accelerated motion. Its transverse intensity distribution is invariant but it propagates on a parabolic trajectory. Three decades later, Siviloglou and co-workers demonstrated theoretically and experimentally this kind of propagation-invariant beam [2]. The self-healing Airy beam [3] paved the way for applications of accelerating beams. Subsequently, a whole family of accelerating beams were discovered, including paraxial [4], non-paraxial [5], truncated by Laguerre- and Hermite-Gaussian beams and thus of finite energy [6]. This property of beam acceleration is useful in many applications such as light sheet microscopy [7], optical routing [8], micro-manipulation [9] and micro-machining [10]. On one hand, these engineered beams exhibit complex bendings of their trajectories, and thus require phase structures. These in turn demand either, extended optical systems, or dynamic optical elements such as a spatial light modulator (SLM) or a digital micromirror device (DMD). Such devices impede urgently needed integrated and miniaturized experimental systems [11]. Furthermore, a direct generation of the Airy beam requires encoding a 3/2 phase pattern into an SLM [12,13], and was later generalized to include arbitrary convex accelerating beams [14].

#453593 https://doi.org/10.1364/OE.453593
Journal © 2022 Received 14 Jan 2022; revised 15 Feb 2022; accepted 17 Feb 2022; published 12 May 2022

Optics EXPRESS

However, these phase patterns consist of complicated phase functions and needs continuous phase modulation, and they can be limiting in practice due to the difficult and demanding techniques to fabricate them by optical phase plates.

On the other hand, diffractive optical elements (DOEs) or meta-surfaces are useful tools for beam shaping, such as tailoring the beam propagation properties in terms of robust phase masks [15–17]. They imprint complex spatial phase distributions to incident beams, however consist of substructures, which are challenging to be fabricated [18]. Another limiting factor of these DOEs arises from poor diffraction efficiency since the intensity of light needs to be directed into a particular diffraction order.

One point of interest is the utility of a simple binary phase patterns, namely a phase slit or a $\pi$ phase step to split an incident beam into two beamlets having opposite direction to transform the optical beam into a desired shape. It has already been proposed numerically and experimentally in several studies [19,20]. Apart from their simple structures, the interest on these phase profiles was mainly driven by their relatively easy fabrication as DOEs which require only two phase levels, and they were mainly investigated as beam shapers to generate a flat-top beam. In addition, several studies demonstrated that the intensity maxima of light diffracted by a straight amplitude edge or a corner propagate along a parabolic trajectory, and the generation of a curved laser microjet using a phase glass corner was demonstrated experimentally [21–23]. However, the generation of an accelerating beam using a $\pi$ phase step or a phase slit has not yet been realized although it would have strong implications in industrial and rugged environments.

In light of these studies, employing a $\pi$ phase step or a $\pi$ phase slit patterns to a Gaussian beam, we are able to generate a tunable accelerating beams which we call Dual Projectile Beams (DPB). Note that, the term "accelerating" in this context is used in a more general sense, which is manifested by propagation of the light beam in a curved manner, i.e. the beam exhibits both negative and positive accelerations during propagation [23]. Combining these phase structures with a lens function with different focal lengths can be regarded as an alternative means to generate adaptive curved laser beams in a significantly easier manner compared to other accelerating beams. Especially that, generating accelerating beams with different trajectories and precise control over their paths requires usually an extended setup with dynamic optical elements [24], or some advanced techniques such as holography methods [25].

DPBs are practical complements to more complex accelerating beams. The simplicity of the applied binary phase patterns and their ability to directly generate an accelerating beam is the key to provide highly advanced and structured light fields in various photonics. This can be crucial in integrated optics where the system design requires thinner and lighter optical elements with high quality standards. We employ a $\pi$ phase step function $\tau_1(x, y)$ illuminated by a fundamental Gaussian beam to generate a hollow core DPB by means of destructive interference (see Fig. 1(a)), and a $\pi$ phase slit $\tau_2(x, y)$ to generate abruptly auto-focusing beam with a bright spot at the central focus. In addition, adding a lens function with different focal lengths allows for a dynamic control of the beam curvature and hence the controlling of the auto-focusing position of the beam. In contrast to other dynamic devices such as a DMD, the advantage of adding a lens to dynamically control the beam trajectory is motivated by the reduction of the complexity, size and weight of the system. Finally, we present the functionality of the approach exemplary using a spatial light modulator (SLM). However, we emphasize that the beam generating phase pattern can easily be fabricated as static refractive or diffractive optical elements, e.g. fabricated by lithography, etching, Or they can also be realized as ultra-thin metasurfaces [11] . This is beneficial for high-power applications, since other phase patterns are often challenging to fabricate because they require multiple phase levels, and are costly.

As a practical example of the potential of the DPBs, we exploit their abruptly auto-focusing property by the formation of a spatial soliton in a nonlinear photorefractive medium. Previous works that base on accelerating beams for soliton formation required complex beam shaping

Optics EXPRESS

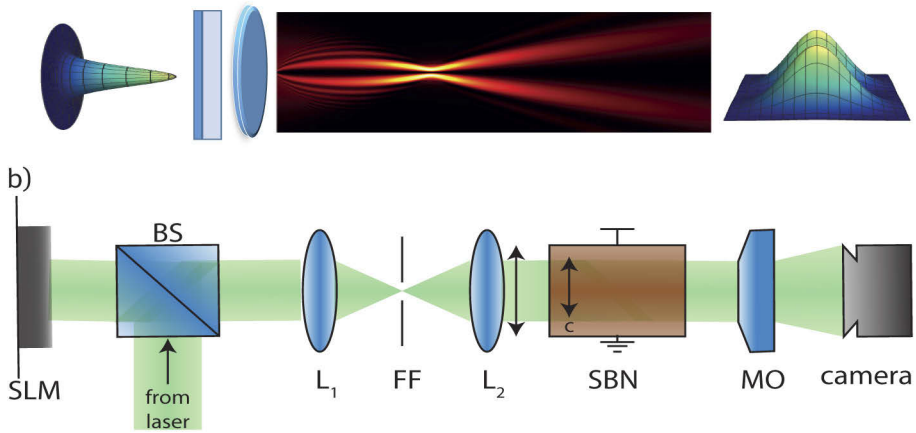


**Fig. 1.** Principe of DPB generation: (a) Conversion of a Gaussian beam into DPB by a DOE which splits the beam into two beamlets that propagate parabolically. (b) Experimental configuration used for beam generation (SLM: Spatial Light Modulator, BS: beam splitter, FF: Fourier filter, SBN: strontium barium niobate crystal, MO: microscope objective).

where adjustment and calibration is crucial since multiple beams are required which is not the case with the presented beam [26–28]. Furthermore, the generation of curved laser beams by diffraction at an edge of an opaque screen or by a corner phase step [21–23] has been investigated only in free space so far. Investigating the dynamics of the studied beam in a nonlinear medium opens new avenues to control the acceleration of light beams such as the suppressing of the beam acceleration. As a key feature, the beam propagates in these materials in a solitary way, thus exhibiting almost no changes in diameter for very long propagation distances.

## 2. Theoretical model and experimental system

To realize DPBs, we consider two simple phase functions which modulate a fundamental Gaussian beam $\psi(r) = \exp\left[-r^2/w_0^2\right]$, where $r = \pm\sqrt{x^2 + y^2}$ is the radial coordinate and $w_0$ is the beam waist. The phase functions $\tau$ are described by

$$\tau_1(x, y) = \begin{cases} 1 & x \geq 0 \\ \exp(\mathrm{i}\pi) & x<0 \end{cases}, \tag{1}$$

and

$$\tau_2(x, y) = \begin{cases} \exp(\mathrm{i}\pi) & |\, x\,| < a/2 \\ 1 & |\, x\,| \geq a/2 \end{cases}, \tag{2}$$

$\tau_1(x, y)$ describes a $\pi$ phase step and $\tau_2(x, y)$ a $\pi$ phase slit with a width of $a$. Both functions modulate the beam in $x$-direction, while it remains unchanged in the $y$-direction. The trajectories of the DPBs and their focusing behavior can be controlled by additional focusing with different focal lengths $f$. Therefore, we modify the transmission functions by corresponding Fresnel lenses that obey $\exp\left[-\mathrm{i}k/(2f)(x^2 + y^2)\right]$ as illustrated in the generation scheme in Fig. 1(a).

Optics EXPRESS

Using the Kirchhoff-Fresnel integral [21], we calculate an analytical expression for the propagation of DPB exemplary for the $\pi$ step phase

$$\begin{aligned} E(x,y,z) &= \frac{k}{2\pi \mathrm{i}z}\int_{\mathbb{R}^2} \tau_1(x',y') e^{-\mathrm{i}\frac{k}{2f}(x'^2+y'^2)} e^{-(x'^2+y'^2)/w_0^2} \\ &\times e^{\mathrm{i}\frac{k}{2z}[(x-x')^2+(y-y')^2]} \mathrm{d}x'\mathrm{d}y' \\ &= \frac{-z_e}{\mathrm{i}\beta z}\exp\left[-\frac{z_e^2}{\beta z^2}\frac{r^2}{w_0^2}\right]\exp\left[\mathrm{i}\frac{z_e}{z}\frac{r^2}{w_0^2}\right]\mathrm{erf}\left[\mathrm{i}\frac{z_e}{\sqrt{\beta}z}\frac{x}{w_0}\right], \end{aligned} \tag{3}$$

where $z_e = k_0 w_0^2/2$ is the Rayleigh distance and $\beta = 1 + \mathrm{i}z_e/f - \mathrm{i}z_e/z$ is a scaling factor that depends on the propagation distance $z$ and focal length $f$. Note that a system without any focusing is described by $f \to \infty$.

We simulate the propagation of the linearly polarized, paraxial Gaussian beams $\psi(\mathbf{r})$ modulated by the phase functions in free-space and demonstrate their nonlinear self-focusing towards soliton formation in a photorefractive medium. For the simulations, we solve the nonlinear Schrödinger equation (NLSE) [27]

$$\mathrm{i}\partial_z\psi(\mathbf{r}) + \frac{\nabla_\perp^2}{2n_e k_0}\psi(\mathbf{r}) + \frac{k_0\Delta n(I)}{2n_e}\psi(\mathbf{r}) = 0, \tag{4}$$

using a spectral split step algorithm [29]. Here $k_0 = 2\pi/\lambda_0$ is the vacuum wave number, related to the wavelength $\lambda_0$. The extraordinarily polarized light field addresses the bulk refractive index $n_e = 2.358$. The spatially varying incident intensity $I(\mathbf{r}) = |\psi(\mathbf{r})|^2$ induces a Kerr-like but saturable refractive index modulation $\Delta n(I)$, according to the photorefractive effect [30].

As a consequence of the incident intensity $I$, an internal electric space charge field $E_{\mathrm{sc}}$ forms in the presence of the external electric bias $E_{\mathrm{ext}}$. The resulting refractive index modulation is described by the Pockels effect $\Delta n = 1/2 n_e^3 r_{33} E_{\mathrm{sc}}$. We calculate the space charge field $E_{\mathrm{sc}} = \partial_x \phi_{\mathrm{sc}}$ solving the equation

$$\Delta_\perp \phi_{\mathrm{sc}} + \nabla_\perp \ln(1+\mathcal{I}) \cdot \nabla_\perp \phi_{\mathrm{sc}} = E_{\mathrm{ext}} \partial_x \ln(1+\mathcal{I}), \tag{5}$$

for the potential $\phi_{\mathrm{sc}}$ [31]. Note that $\mathcal{I} = I/I_{\mathrm{sat}}$ is a normalized intensity used in the simulations that takes into account an empiric saturation intensity $I_{\mathrm{sat}}$, which results due to thermal excitations as a dark current intensity and can be determined experimentally [32].

We generate DPBs using the experimental system shown in Fig. 1(b). The collimated and expanded cw laser beam of a frequency-doubled Nd:$YVO_4$ laser with a wavelength of $\lambda_0 = 532$nm is spatially modulated by a phase-only SLM, 'Holoeye Pluto VIS', both in amplitude and phase, using a pre-encoded hologram and a Fourier space filtering (FF) [33].

The SLM acts as the desired phase transmittance by imprinting the phases $\tau$ onto the incident Gaussian beams. The free-space propagation of the spatially structured beam is analyzed using a microscope objective that can be shifted in propagation direction by the telescope system $L_1$ - $L_2$ (10x demagnification) and a camera. For soliton formation, a photorefractive cerium-doped strontium barium niobate crystal (SBN:Ce) is included in the system, whose front face is placed at the image plane of the SLM. The 20 mm long crystal is externally biased with an electric field $E_{\mathrm{ext}} = 2000\,\mathrm{V/cm}$ along its optical $c$-axis, parallel to the $x$-axis, in order to enhance the refractive index modulation [31]. The extraordinary polarized light field addresses the stronger electro-optic coefficient $r_{33} = 237\,\mathrm{pmV}^{-1}$ of the birefringent SBN crystal [27].

## 3. Generation of DPBs and nonlinear photonic structures

### 3.1. Propagation of the DPBs in free-space

First, to demonstrate the trajectory of the DPB, Fig. 2 represents the 2D transverse profile (Fig. 2(a)) and the propagation of the beam according to Eq. (3). As seen in Fig. 2(b), the two

Optics EXPRESS

intensity maxima of the DPB follows a root parabolic trajectory, i.e. $x = C\sqrt{z}$, as indicated by the dashed line in Fig. 2(b).

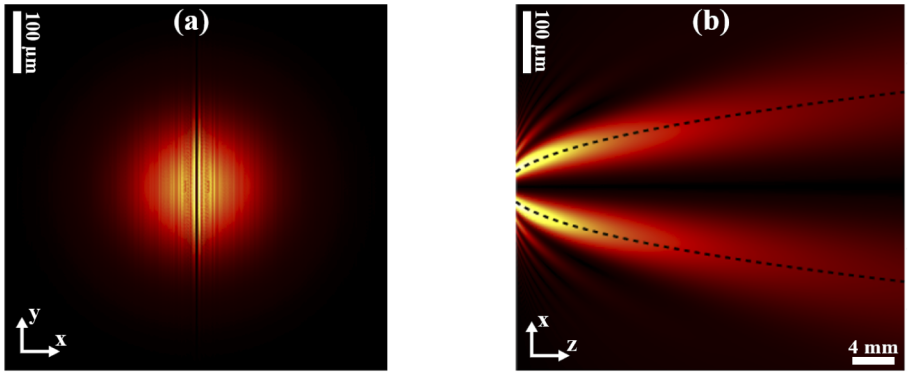


**Fig. 2.** (a) 2D transverse (x,y) profile of DPB. (b) propagation of the beam in z-direction. The dashed curve depicts the acceleration of the two intensity maxima.

Next, we generate a DPB using a $\pi$ phase step $\tau_1$ without focusing. Its simulated (top) and experimentally observed (bottom) transverse intensity distributions at different $z$-positions and a $xz$-cross-section through the intensity volume during propagation are shown in Fig. 3.

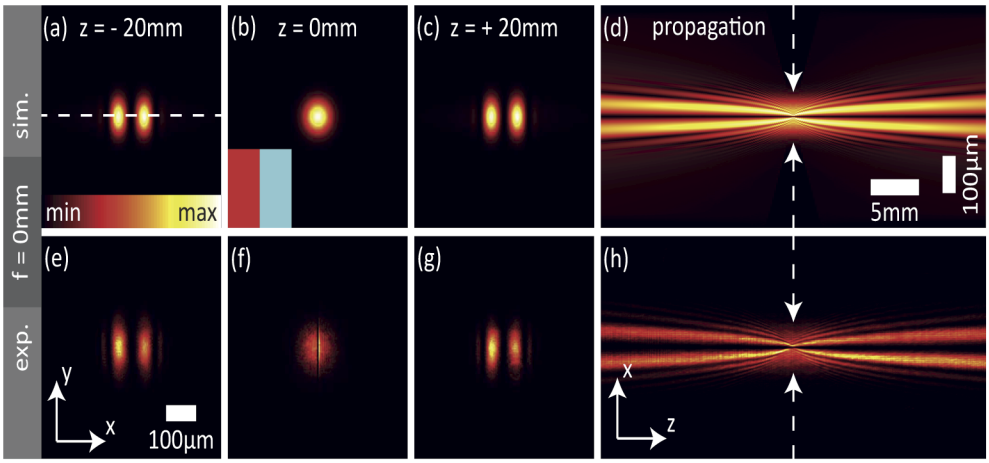


**Fig. 3.** Evolution of the transverse (a-c, e-g) and longitudinal (d and h) intensity distributions of DPB for the $\pi$ phase step: simulation (top row) and experiment (bottom row).

We show transverse intensity distributions (Figs. 3(a)–3(c), 3(e)–3(g)) at the origin at $z = 0$ mm and symmetrically at $z = \pm 20$ mm. It is worth noting that the SLM image plane is referred to as $z = 0$ mm, and the intensity distributions are obtained by moving the image plane forwards (positive z) and backwards (negative z). Without any focusing, the light propagation is symmetric along $z$-direction . The origin at $z = 0$ mm shows the initial Gaussian beam with a waist of $w_0 = 100\ \mu$m. The small inset represents a color-coded phase distribution with a $\pi$ jump. The evolution of the beam along the propagation direction is imaged in experiments by recording 400 intensity profiles at equidistant transverse planes in the range of $z = -20$ to $+20$ mm. Though the beam is measured in free-space, these longitudinal distances refer to the propagation distances in the SBN crystal with a refractive index of $n_e$, since we adopt the beam sizes for the later shown soliton formation. Since some of the DPBs have focal peak intensities that are two magnitudes

Optics EXPRESS

higher than the initial intensity, for all $xz$-cross-sections that show the propagation of the beams, we show the square root of the intensity to increase the visibility of the beam trajectories. The parabolic trajectory nature and the zero on-axis intensity are shown in Figs. 3(d) and 3(h).

In the same manner, Fig. 4 depicts the numerical simulation (top) and the corresponding experimental results (bottom), respectively, for a Gaussian beam with an initial beam size of $w_0 = 100\,\mu$m and a phase slit width of $a = 20\,\mu$m. We show the transverse intensity distributions (Figs. 4(a)–4(c), 4(e)–4(g)) of the DPB at $z = \pm 20$ mm and in the initial plane at $z = 0$ mm as well as the $xz$-cross-section at $y = 0\,\mu$m through the intensity volume of the evolution of the beam (Figs. 4(d) and 4(h)).

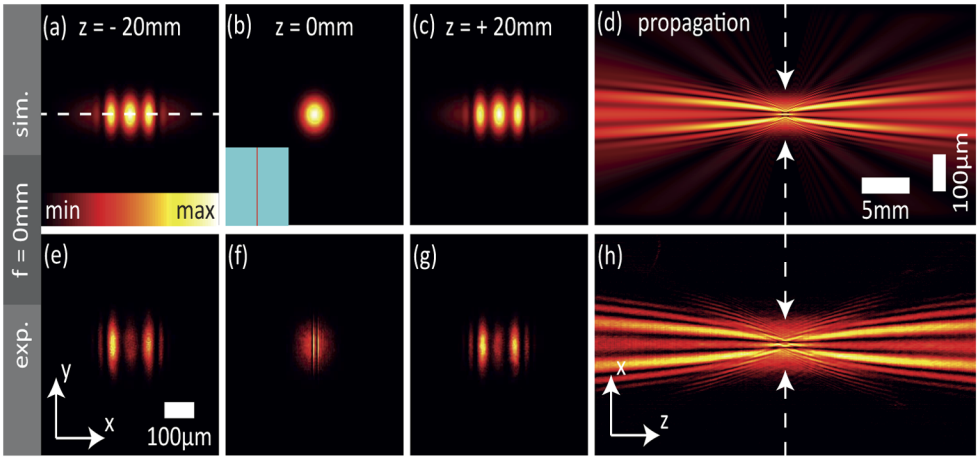


**Fig. 4.** Evolution of the transverse (a-c, e-g) and longitudinal (d and h) intensity distributions of DPB for the slit phase: simulation (top row) and experiment (bottom row).

Generating DPBs using a phase slit presents an attractive possibility to form a high-intensity spot at the intersection position of the two focusing sides of the beam at the focus plane due to constructive interference. That reveals the auto-focusing property of the beam. Similarly to radially symmetric abruptly focusing Airy beams [26,34,35], the intensity maxima of DPBs propagate on a parabolic trajectory towards the focus and undergo a sudden increase of their intensity near the focal point. This abrupt auto-focusing is highly advantageous in many applications of material processing and particle manipulation [7,10,26].

### 3.2. Controlling the curvatures of DPBs

Being able to change the longitudinal intersection position of the two sides of the DPBs, and hence the auto-focusing of the beams can be crucial for the named applications. Here, we achieve this aim using Fresnel lenses with different focal lengths $f$ as additional phase modulations. Figure 5 shows the effect of the focusing with exemplary focal lengths of $f = 5$ mm and $f = 10$ mm, respectively, on the beam curvature. Like before, we scan the intensity volume in a range of $z = -20$ mm to $+20$ mm. Due to the strong focusing of the beam, the dynamic range covered by the whole $xz$-cross-section reaches the detection limits of the camera. To obtain the cross-sections with a good signal-to-noise ratio, we average each transverse intensity distribution over 20 measurements, which decreases the individual exposure time to an acceptable level so that we are able to observe the beam propagation evolution the $xz$-cross-section.

The transverse intensity distributions (Figs. 5(a), 5(c), 5(e), 5(g), 5(i), 5(k), 5(m), and 5(o)) at $\pm 20$ mm are asymmetric due to the asymmetric focusing effects. Figures 5(b), 5(f), 5(j) and 5(n) show the transverse intensity distributions in the respective focal plane. Demonstrated by the $xz$-cross-sections of the intensity during propagation, we control the trajectories of the

Optics EXPRESS

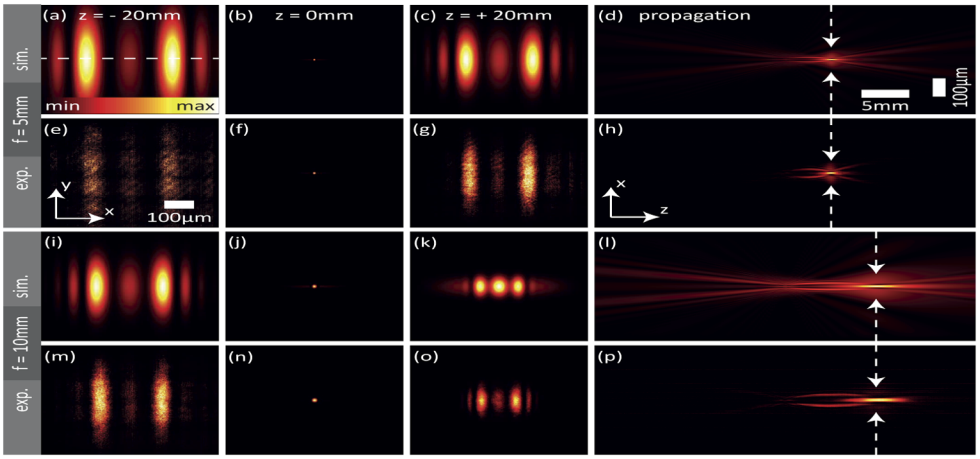


**Fig. 5.** Evolution of the transverse (a-c, e-f, i-k, m-o) and longitudinal (d, h, l and p) intensity distributions when manipulating the DPB trajectory. Simulation for lenses of $f = 5$ mm and $f = 10$ mm respectively (first and third rows). Corresponding experiment results (second and fourth rows).

two parabolically propagating maxima of the beams and consequently the focal positions of the elongated intensity spots, which are indicated by white dashed arrows (Figs. 5(d), 5(h), 5(l) and 5(p)). Due to the abrupt focusing, the beams' intensity is mainly visible close to the focal point though the visualization uses the square root of the intensity. Comparing the maximum intensity at the initial plane at $z = 0$ mm with the maximum intensity in the respective focal plane, we find an increase of a factor of $37.0 \pm 1.7$ ($f = 5$ mm, sim.), $263.2 \pm 9.2$ ($f = 5$ mm, exp.), $9.3 \pm 0.8$ ($f = 10$ mm, sim.), $88.3 \pm 4.8$ ($f = 10$ mm, exp.). The simulated and experimentally obtained results are qualitatively in good agreement, but differ quantitatively, because the areas of the SLM and the simulated counterpart are not identical.

### 3.3. *Exploiting DPBs for soliton formation in nonlinear media*

Previous studies carried out with Airy and other accelerating beams showed that the interaction of light propagating on two converging parabolic paths leads to spatial soliton formation in focusing nonlinear media [27,28,36]. The focusing and saturable nonlinearity of the SBN crystal manifests in the increased refractive index modulation that in turn alters the light propagation. Using constructively interfering DPB produced by a $\pi$ phase slit $\tau_2$ and a focal length of $f = 5$ mm, we analyze the dynamics of the beam in the nonlinear medium, capable of forming a spatial soliton. Note that this DPB has a beam waist of $w_0 = 4\,\mu$m in its focal plane at $z = 5$ mm and thus a Rayleigh length of $z_e \approx 95\,\mu$m.

The experimental and the numerical results are shown in Fig. 6. For an adequate beam power of $P \approx 10\,\mu$W, the focal intensity forms a self-focusing refractive index modulation at the longitudinal position where the beam focuses spontaneously, at $z = 5$ mm. The intensity exactly compensates the beams' diffraction, leading to a localized intensity mode that continues propagating as a soliton of a diameter $w_0 \approx 4\mu m$. As a glance inside the non-homogeneous medium is not possible directly, we image the output face of the SBN crystal experimentally and compare the results with numerical simulations [27,28]. The simulations predict the dynamics of the beam inside the crystal, revealing that the beam propagates almost unchanged, as shown with the transverse intensity distributions related to different planes indicated by white, dashed arrows. The lower row of Fig. 6 represents the numerically calculated refractive index modulations at the respective plane. The simulations and experiment calculations are in good agreement.

Optics EXPRESS

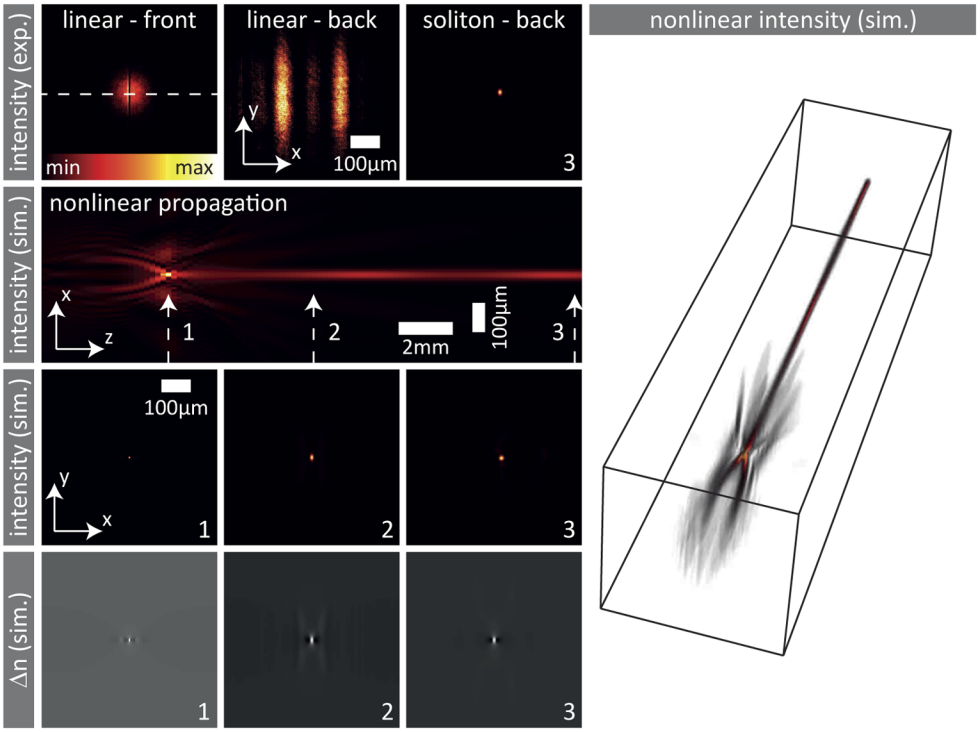


**Fig. 6.** Soliton formation using DPB. Experimental results for the transverse intensity distribution in the linear and nonlinear regimes (top row). Simulations of longitudinal evolution of DPB and transverse intensity distributions in a non-linear regime and the corresponding refractive index modulation (second to fourth rows). 3D volumetric rendering simulation of intensity distribution.

The soliton formation process during the nonlinear propagation of the beam can be clearly seen in the volumetric rendering of the numerically simulated intensity distribution. Although modulations are present around the localized solitary state, which is due to the interference with secondary side lobes of the beam, in general the localized mode propagates almost unchanged to the end of crystal. This distance corresponds to $\approx$ 158 Rayleigh lengths. The interaction of the two sides of the DPB in the presence of such a photorefractive nonlinearity leads to the suppression of its parabolic trajectory. This confinement can be regarded to as beam deceleration, and was discussed in earlier studies [6,27].

## 4. Conclusion

In conclusion, we demonstrated numerically and experimentally a simple and direct approach to generate tunable accelerating beams. In comparison to other accelerating beams that require complex phase patterns to be generated and are limited in practice, DPBs are easy to implement and might be generated using simple DOEs which are energy robust and intensity efficient, and can also be an advantage especially meeting the demand for miniaturized optical systems and integrated optics. The propagation analysis of DPB in a linear regime showed different scenarios at the intersection plane of the two beam sides in which they interfere destructively resulting in a hollow beam or interfere constructively resulting in bright intensity spot accounting for an abrupt auto-focusing of the beam. Also, we showed that a full control over the curvature of the beam is possible by adding a focusing with different focal lengths. Furthermore, we studied the nonlinear

Optics EXPRESS

dynamics of DPB inside a photorefractive SNB crystal. We demonstrated that the nonlinear refractive index changes alter the dynamic of DPBs substantially and give rise to properties such as deceleration of the beam and generation of a localized solitary state. We believe that DPBs serve as a simple toolbox to study accelerating beams and prepare them for many applications.

**Funding.** Direction Générale de la Recherche Scientifique et du Développement Technologique; Institute of Optics and Precision Mechanics (UFAS1); Deutscher Akademischer Austauschdienst; Westfälische Wilhelms-Universität Münster.

**Disclosures.** The authors declare no conflicts of interest.

**Data availability.** Data underlying the results presented in this paper are not publicly available at this time but may be obtained from the authors upon reasonable request.

## References

1. M. V. Berry and N. L. Balazs, "Nonspreading wave packets," Am. J. Phys. **47**(3), 264–267 (1979).
2. G. A. Siviloglou and D. N. Christodoulides, "Accelerating finite energy airy beams," Opt. Lett. **32**(8), 979–981 (2007).
3. J. Broky, G. A. Siviloglou, A. Dogariu, and D. N. Christodoulides, "Self-healing properties of optical airy beams," Opt. Express **16**(17), 12880–12891 (2008).
4. M. A. Bandres, "Accelerating parabolic beams," Opt. Lett. **33**(15), 1678–1680 (2008).
5. P. Zhang, Y. Hu, T. Li, D. Cannan, X. Yin, R. Morandotti, Z. Chen, and X. Zhang, "Nonparaxial mathieu and weber accelerating beams," Phys. Rev. Lett. **109**(19), 193901 (2012).
6. V. V. Kotlyar, A. A. Kovalev, and V. A. Soifer, "Transformation of decelerating laser beams into accelerating ones," J. Opt. **16**(8), 085701 (2014).
7. T. Vettenburg, H. I. Dalgarno, J. Nylk, C. Coll-Lladó, D. E. Ferrier, T. Čižmár, F. J. Gunn-Moore, and K. Dholakia, "Light-sheet microscopy using an airy beam," Nat. Methods **11**(5), 541–544 (2014).
8. P. Rose, F. Diebel, M. Boguslawski, and C. Denz, "Airy beam induced optical routing," Appl. Phys. Lett. **102**(10), 101101 (2013).
9. J. Baumgartl, M. Mazilu, and K. Dholakia, "Optically mediated particle clearing using airy wavepackets," Nat. Photonics **2**(11), 675–678 (2008).
10. F. Courvoisier, R. Stoian, and A. Couairon, "Ultrafast laser micro- and nano-processing with nondiffracting and curved beams," Opt. Laser Technol. **80**, 125–137 (2016).
11. N. Yu and F. Capasso, "Flat optics with designer metasurfaces," Nat. Mater. **13**(2), 139–150 (2014).
12. D. M. Cottrell, J. A. Davis, and T. M. Hazard, "Direct generation of accelerating airy beams using a 3/2 phase-only pattern," Opt. Lett. **34**(17), 2634–2636 (2009).
13. J. A. Davis, M. J. Mitry, M. A. Bandres, I. Ruiz, K. P. McAuley, and D. M. Cottrell, "Generation of accelerating airy and accelerating parabolic beams using phase-only patterns," Appl. Opt. **48**(17), 3170–3176 (2009).
14. L. Froehly, F. Courvoisier, A. Mathis, M. Jacquot, L. Furfaro, R. Giust, P. A. Lacourt, and J. M. Dudley, "Arbitrary accelerating micron-scale caustic beams in two and three dimensions," Opt. Express **19**(17), 16455–16465 (2011).
15. N. Yu, P. Genevet, M. A. Kats, F. Aieta, J.-P. Tetienne, F. Capasso, and Z. Gaburro, "Light propagation with phase discontinuities: Generalized laws of reflection and refraction," Science **334**(6054), 333–337 (2011).
16. A. Bencheikh, M. Fromager, and K. A. Ameur, "Generation of Laguerre-Gaussian LG_p0 beams using binary phase diffractive optical elements," Appl. Opt. **53**(21), 4761 (2014).
17. B. Abdelhalim, M. Fromager, and K. A. Ameur, "Extended focus depth for gaussian beam using binary phase diffractive optical elements," Appl. Opt. **57**(8), 1899–1903 (2018).
18. M. Taghizadeh, P. Blair, B. Layet, I. Barton, A. Waddie, and N. Ross, "Design and fabrication of diffractive optical elements," Microelectron. Eng. **34**(3-4), 219–242 (1997).
19. W. B. Veldkamp and C. J. Kastner, "Beam profile shaping for laser radars that use detector arrays," Appl. Opt. **21**(2), 345–356 (1982).
20. N. Passilly, M. Fromager, L. Mechin, C. Gunther, S. Eimer, T. Mohammed-Brahim, and K. Aït-Ameur, "1-d laser beam shaping using an adjustable binary diffractive optical element," Opt. Commun. **241**(4-6), 465–473 (2004).
21. M. Born and E. Wolf, *Principles of Optics* (Pergamon Press, 1970), 4th ed.
22. V. V. Kotlyar, S. S. Stafeev, and A. A. Kovalev, "Curved laser microjet in near field," Appl. Opt. **52**(18), 4131–4136 (2013).
23. Y. Zhang, M. R. Belić, H. Zheng, Z. Wu, Y. Li, K. Lu, and Y. Zhang, "Fresnel diffraction patterns as accelerating beams," EPL **104**(3), 34007 (2013).
24. S. Vo, K. Fuerschbach, K. P. Thompson, M. A. Alonso, and J. P. Rolland, "Airy beams: a geometric optics perspective," J. Opt. Soc. Am. A **27**(12), 2574–2582 (2010).
25. T. Latychevskaia and H.-W. Fink, "Inverted Gabor holography principle for tailoring arbitrary shaped three-dimensional beams," Sci. Rep. **6**, 26312 (2016).
26. N. K. Efremidis and D. N. Christodoulides, "Abruptly autofocusing waves," Opt. Lett. **35**(23), 4045–4047 (2010).
27. F. Diebel, B. M. Bokić, D. V. Timotijević, D. M. J. Savić, and C. Denz, "Soliton formation by decelerating interacting airy beams," Opt. Express **23**(19), 24351–24361 (2015).

Optics EXPRESS


28. A. Zannotti, M. Rüschenbaum, and C. Denz, "Pearcey solitons in curved nonlinear photonic caustic lattices," J. Opt. **19**(9), 094001 (2017).
29. G. Agrawal, *Nonlinear Fiber Optics* (Academic Press, 2013), 5th ed.
30. N. Kukhtarev, V. Markov, S. Odulov, M. Soskin, and V. Vinetskii, "Holographic storage in electrooptic crystals. I. steady state," Ferroelectrics **22**(1), 949–960 (1979).
31. A. A. Zozulya and D. Z. Anderson, "Propagation of an optical beam in a photorefractive medium in the presence of a photogalvanic nonlinearity or an externally applied electric field," Phys. Rev. A **51**(2), 1520–1531 (1995).
32. M. Segev, "Optical Spatial Solitons," Opt. Quantum Electron. **30**(7/10), 503–533 (1998).
33. J. A. Davis, D. M. Cottrell, J. Campos, M. J. Yzuel, and I. Moreno, "Encoding amplitude information onto phase-only filters," Appl. Opt. **38**(23), 5004–5013 (1999).
34. A. Bencheikh, "Spatial characteristics of the truncated circular Airyprime beam," Opt. Quantum Electron. **51**(1), 2–11 (2019).
35. A. Bencheikh, "Airyprime beam: From the non-truncated case to truncated one," Optik **181**, 659–665 (2019).
36. Y. Zhang, M. Belić, Z. Wu, H. Zheng, K. Lu, Y. Li, and Y. Zhang, "Soliton pair generation in the interactions of airy and nonlinear accelerating beams," Opt. Lett. **38**(22), 4585–4588 (2013).